2546–2559 Nucleic Acids Research, 2019, Vol. 47, No. 5 Published online 19 December 2018
doi: 10.1093/nar/gky1266

The Tudor protein Veneno assembles the ping-pong amplification complex that produces viral piRNAs in *Aedes* mosquitoes

Joep Joosten[1], Pascal Miesen[1], Ezgi Taşköprü[1], Bas Pennings[1], Pascal W.T.C. Jansen[2], Martijn A. Huynen[3], Michiel Vermeulen[2] and Ronald P. Van Rij[1,*]

[1]Department of Medical Microbiology, Radboud Institute for Molecular Life Sciences, Radboud University Medical Center, P.O. Box 9101, 6500 HB Nijmegen, The Netherlands, [2]Department of Molecular Biology, Faculty of Science, Radboud Institute for Molecular Life Sciences, Oncode Institute, Radboud University Nijmegen, P.O. Box 9101, 6500 HB Nijmegen, The Netherlands and [3]Center for Molecular and Biomolecular Informatics, Radboud Institute for Molecular Life Sciences, Radboud University Medical Center, P.O. Box 9101, 6500 HB Nijmegen, The Netherlands

Received October 24, 2018; Revised November 28, 2018; Editorial Decision December 04, 2018; Accepted December 10, 2018

ABSTRACT

PIWI-interacting RNAs (piRNAs) comprise a class of small RNAs best known for suppressing transposable elements in germline tissues. The vector mosquito *Aedes aegypti* encodes seven PIWI genes, four of which are somatically expressed. This somatic piRNA pathway generates piRNAs from viral RNA during infection with cytoplasmic RNA viruses through ping-pong amplification by the PIWI proteins Ago3 and Piwi5. Yet, additional insights into the molecular mechanisms mediating non-canonical piRNA production are lacking. TUDOR-domain containing (Tudor) proteins facilitate piRNA biogenesis in *Drosophila melanogaster* and other model organisms. We thus hypothesized that Tudor proteins are required for viral piRNA production and performed a knockdown screen targeting all *A. aegypti* Tudor genes. Knockdown of the Tudor genes AAEL012437, Vreteno, Yb, SMN and AAEL008101-RB resulted in significantly reduced viral piRNA levels, with AAEL012437-depletion having the strongest effect. This protein, which we named Veneno, associates directly with Ago3 in an sDMA-dependent manner and localizes in cytoplasmic foci reminiscent of piRNA processing granules of *Drosophila*. Veneno-interactome analyses reveal a network of cofactors including the orthologs of the *Drosophila* piRNA pathway components Vasa and Yb, which in turn interacts with Piwi5. We propose that Veneno assembles a multi-protein complex for ping-pong dependent piRNA production from viral RNA.

INTRODUCTION

In animals, three distinct small RNA-mediated silencing pathways exist: the micro (mi)RNA, small interfering (si)RNA and PIWI-interacting (pi)RNA pathways (1). In all three, a small RNA molecule provides sequence specificity to guide a member of the Argonaute protein family to target RNA. Whereas miRNAs and siRNAs associate with proteins of the AGO clade of this family, piRNAs are loaded onto PIWI clade proteins exclusively, forming piRNA induced silencing complexes (piRISCs) (2).

The piRNA pathway is primarily known for its role in transgenerational protection of genome integrity by silencing transposable elements in the germline (3,4). Despite ubiquitous expression of piRNAs across metazoans, our knowledge on the molecular mechanisms that govern the piRNA pathway is limited to only a small number of model organisms (5). In the *Drosophila melanogaster* germline, single-stranded precursors are produced from genomic piRNA clusters that contain remnants of transposable elements (6). These precursors leave the nucleus and are processed to give rise to a pool of primary piRNAs. The PIWI proteins Piwi and Aubergine (Aub) are preferentially loaded with such primary piRNAs that bear a uridine at the first nucleotide position (1U) and are generally antisense toward transposon mRNAs (6–8). Upon loading with a piRNA, Piwi migrates to the nucleus to enforce transcriptional silencing, while Aub targets and cleaves cognate transposon RNA in an electron-dense perinuclear structure termed *nuage* (3,9). The 3′-fragments that remain after Aub-cleavage are subsequently loaded onto the PIWI protein Ago3 and processed further into mature secondary piRNAs, which are primarily of sense orientation (6,7). In

*To whom correspondence should be addressed. Tel: +31243617574; Email: ronald.vanrij@radboudumc.nl

turn, the resulting Ago3-piRISCs can target and cleave precursor transcripts to produce new antisense Aub-associated piRNAs, thus completing the so-called ping-pong amplification cycle. As Aub preferentially binds 1U piRNAs and cleaves target RNAs between nucleotides 10 and 11, Ago3-associated secondary piRNAs mostly have adenosine residues at their tenth nucleotide position (10A). The resulting 10 nt overlap of 5′ ends and 1U/10A nucleotide biases are hallmarks of piRNA production by the ping-pong amplification loop and are referred to as the ping-pong signature (6,7). In addition to ping-pong amplification of piRNAs, Aub- and Ago3-mediated cleavage can induce phased production of downstream Piwi-associated piRNAs that have a strong 1U preference (10,11).

Ping-pong amplification of piRNAs was previously thought to be restricted to germline tissues, but recently, ping-pong dependent piRNA production has been demonstrated in somatic tissues of several arthropods, among which hematophagous mosquitoes of the *Aedes* family (12,13). These vector mosquitoes, primarily *A. aegypti* and *Aedes albopictus*, are crucial for the transmission of several arthropod-borne (arbo)viruses that cause debilitating diseases such as dengue, chikungunya and Zika (14). Since arboviral infectivity is greatly affected by the ability of the virus to replicate in the vector, mosquito antiviral immunity is a key determinant for virus transmission. Intriguingly, while causing severe disease in vertebrate hosts, arboviruses are able to replicate to high levels in the mosquito without apparent fitness cost to the insect (15). An efficient immune response based on small interfering (si)RNAs is thought to contribute to this tolerance phenotype, as genetic interference with viral siRNA production causes elevated virus replication accompanied by increased mosquito mortality (16–19).

In addition to siRNAs, arbovirus infection results in *de novo* production of virus-derived piRNAs (vpiRNAs) in aedine mosquitoes and cell lines, suggesting that two independent small RNA pathways contribute to antiviral immunity in these insects (13). In *A. aegypti* cells, vpiRNAs from the alphavirus Sindbis virus (SINV) are predominantly produced in a ping-pong amplification loop involving the PIWI proteins Ago3 and Piwi5 (20). These proteins associate directly with vpiRNAs, which bear the distinct 1U/10A nucleotide signature indicative of ping-pong amplification. The further configuration of protein complexes responsible for vpiRNA biogenesis is currently unknown. Moreover, it is unclear whether vpiRNA production requires dedicated protein complexes that differ from those that mediate biogenesis of piRNAs from other substrates, such as transposons or host mRNAs.

Studies in *D. melanogaster* and other model organisms have shown that TUDOR domain-containing (Tudor) proteins serve important functions in piRNA biogenesis, including the prevention of non-specific degradation of piRNA substrates, facilitating PIWI protein interactions, and aiding in small RNA loading onto specific PIWI proteins (3,4,21,22). TUDOR domains contain conserved motifs that are known to interact with symmetrically dimethylated arginines (sDMAs), a common post-translational modification on PIWI proteins (23–25). Consequently, Tudor proteins may serve as adaptor molecules that assemble multi-molecular complexes involved in vpiRNA biogenesis in *A. aegypti*.

To test this hypothesis, we performed a functional knockdown screen of all predicted *A. aegypti* Tudor proteins, in which knockdown of the hitherto uncharacterized Tudor protein AAEL012437 shows the most prominent vpiRNA depletion. Because of this dramatic effect on vpiRNA biogenesis and the fact that its direct *D. melanogaster* ortholog (CG9684) is largely uncharacterized, we decided to focus our attention on this protein, which we named Veneno (Ven). Ven-depletion dramatically reduces piRNA production from both viral RNA strands, while ping-pong dependent piRNA production from endogenous sources (Ty3-gypsy transposons and histone H4 mRNA) is only mildly affected. Ven resides in cytoplasmic foci, reminiscent of piRNA processing granules in *Drosophila* and interacts directly with Ago3 through canonical TUDOR domain-mediated sDMA recognition. In addition, Ven associates with orthologs of *Drosophila* piRNA pathway components Vasa (AAEL004978) and Yb (AAEL001939) (9,26–31), which in turn binds Piwi5. We propose that this complex supports efficient ping-pong amplification of vpiRNAs by the PIWI proteins Ago3 and Piwi5.

MATERIALS AND METHODS

Tudor gene identification and ortholog detection

To allow comprehensive identification of all *A. aegypti* Tudor genes, we combined HHpred homology detection with Jackhmmer iterative searches (32,33). Subsequently, identified sequences were aligned using T-Coffee to determine orthologous relations between *A. aegypti* and *D. melanogaster* Tudor proteins (34). In view of the length of the TUDOR domain (∼50 AA) and low levels of sequence conservation among the family members, neighbor joining was used to identify orthology relations, which were consistent with the domain organization of the proteins. See Supplementary Data for a detailed description of our approach.

Transfection and infection of Aag2-cells

In knockdown experiments, cells were transfected with dsRNA and re-transfected 48 h later to ensure prolonged knockdown. Where indicated, cells were infected with a recombinant SINV expressing GFP from a duplicated subgenomic promoter (SINV-GFP; produced from pTE3′2J-GFP (35,36)) at a multiplicity of infection (MOI) of 1 and harvested 48 h post-infection. For immunofluorescence (IFA) and immunoprecipitation (IP) experiments, Aag2 cells were transfected with expression plasmids encoding tagged transgenes and, where indicated, infected with SINV (produced from pTE3′2J (35)) at an MOI of 1, 3 h after transfection. All samples were harvested 48 hours after transfection. For mass spectrometry (MS) experiments, expression plasmids were transfected into cells using polyethylenimine (PEI) and infected 24 hours later with SINV at an MOI of 0.1. MS-samples were harvested 72

hours post-infection. For a more detailed description of cell culture conditions, generation of stable cell lines, generation of expression vectors and virus production, see Supplementary Data.

Small RNA northern blotting and RT-qPCR

For small RNA northern blotting, RNA was size separated on polyacrylamide gels and cross-linked to nylon membranes using 1-ethyl-3-(3-dimethylaminopropyl)carbodiimide hydrochloride (37). Small RNAs were detected using ^{32}P-labeled DNA oligonucleotides. For real-time quantitative polymerase chain reaction (RT-qPCR) analyses, DNaseI-treated RNA was reverse transcribed and PCR amplified in the presence of SYBR green. See Supplementary Data for a detailed description of the experimental procedures and sequences of qPCR primers and probes used for northern blotting.

Preparation of small RNA libraries and bioinformatic analyses

Total RNA from Aag2 cells transfected with dsRNA targeting either Veneno or Firefly Luciferase was used to generate small RNA deep sequencing libraries in parallel. For each condition, three transfections and library preparations were performed. For small RNA-IP libraries, PIWI proteins were immunoprecipitated from SINV-infected Aag2 cell lysates. Purified PIWI protein–piRNA complexes were washed and small RNAs were extracted using proteinase K-treatment. Deep sequencing was performed using Illumina's Truseq technology, as described in (38). See Supplementary Data for a description of the analyses of deep sequencing data.

Fluorescence and microscopy

Fluorescent imaging was performed on paraformaldehyde-fixed Aag2 cells that were permeabilized and counterstained using Hoechst solution. Confocal images were taken using an Olympus FV1000 microscope. Images used for the quantification of GFP-signal granularity were taken using a Zeiss Axio Imager Z1 with ApoTome technology. See Supplementary Data for details of the experimental approach.

Immunoprecipitation and western blotting

GFP- and RFP-tagged transgenes were immunoprecipitated using GFP- and RFP-TRAP beads (Chromotek), respectively, according to the manufacturer's instructions. V5-tagged transgenes were purified using V5-agarose beads (Sigma). For Ago3 and Piwi5 IP experiments, antibodies targeting endogenous proteins were added to lysates at 1:10 dilution and incubated for 4 h at 4°C, followed by overnight binding to Protein A/G PLUS agarose beads (Santa Cruz). Protein extracts were resolved on polyacrylamide gels, blotted to nitrocellulose membranes, and probed with the indicated antibodies. Details on generation of antibodies, experimental procedures, and antibody dilutions can be found in the Supplementary Data.

Mass spectrometry

For MS analysis, precipitated proteins were washed extensively and subjected to on-bead trypsin digestion as described previously (39). Subsequently, tryptic peptides were acidified and desalted using Stagetips (40) before elution onto a NanoLC-MS/MS. Mass spectra were recorded on a QExactive mass spectrometer (Thermo Scientific). For detailed experimental procedures and the analyses of mass spectra, see Supplementary Data.

Density gradient fractionation

Aag2 cell lysate was separated on a 10–45% sucrose gradient by ultracentrifugation. Subsequently, protein was precipitated in acetone and trichloroacetic acid and RNA was extracted using acid phenol/chloroform. For more details, see Supplementary Data.

RESULTS

Comprehensive identification of Tudor proteins in *Aedes aegypti*

Tudor proteins play fundamental roles in the biogenesis of piRNAs in both vertebrate and invertebrate species (21,22). We therefore hypothesized that processing of viral RNA into piRNAs in *A. aegypti* also involves members of this protein family. To faithfully identify all *A. aegypti* Tudor genes and their corresponding fruit fly orthologs, we used a homology-based prediction approach combining HHPred and Jackhmmer algorithms (32,33). First, we used HHPred homology detection to predict *D. melanogaster* TUDOR domain sequences, which were subsequently used as input for Jackhmmer iterative searches to identify all *D. melanogaster* and *A. aegypti* TUDOR domains. Ultimately, a neighbor joining tree was made based on a TUDOR domain alignment generated with T-Coffee (34), which enabled the identification of orthologous relationships between *A. aegypti* and *D. melanogaster* Tudor proteins (Figure 1).

While the bootstrap values suggest relatively low phylogenetic signal in the TUDOR domains themselves, the majority of *A. aegypti* Tudor proteins cluster with a single *D. melanogaster* ortholog with a highly similar domain composition, providing independent support for the orthology relationships. Some genes however (e.g. AAEL022773, AAEL008101, AAEL009987 and AAEL023919) lack clear one-to-one orthology with *Drosophila* counterparts, suggesting that these genes emerged as a result of duplication events that occurred in the *Culicidae* family (mosquitoes). Conversely, CG15042 and Krimper in *D. melanogaster* likely resulted from a duplication in the *Drosophilidae*. Alternatively, the genes without an ortholog may have been lost from the *Drosophila* lineage, or diversified to an extent that they are no longer recognized as orthologs in the multiple sequence alignment. The AAEL008101 gene encodes two splice variants, of which only AAEL008101-PB is expressed in Aag2 cells (Supplementary Figure S1C). Lastly, the *A. aegypti* genome encodes only one ortholog for the *D. melanogaster* Yb protein subfamily (Yb, SoYb and BoYb), namely AAEL001939, which we refer to as Yb. In cases

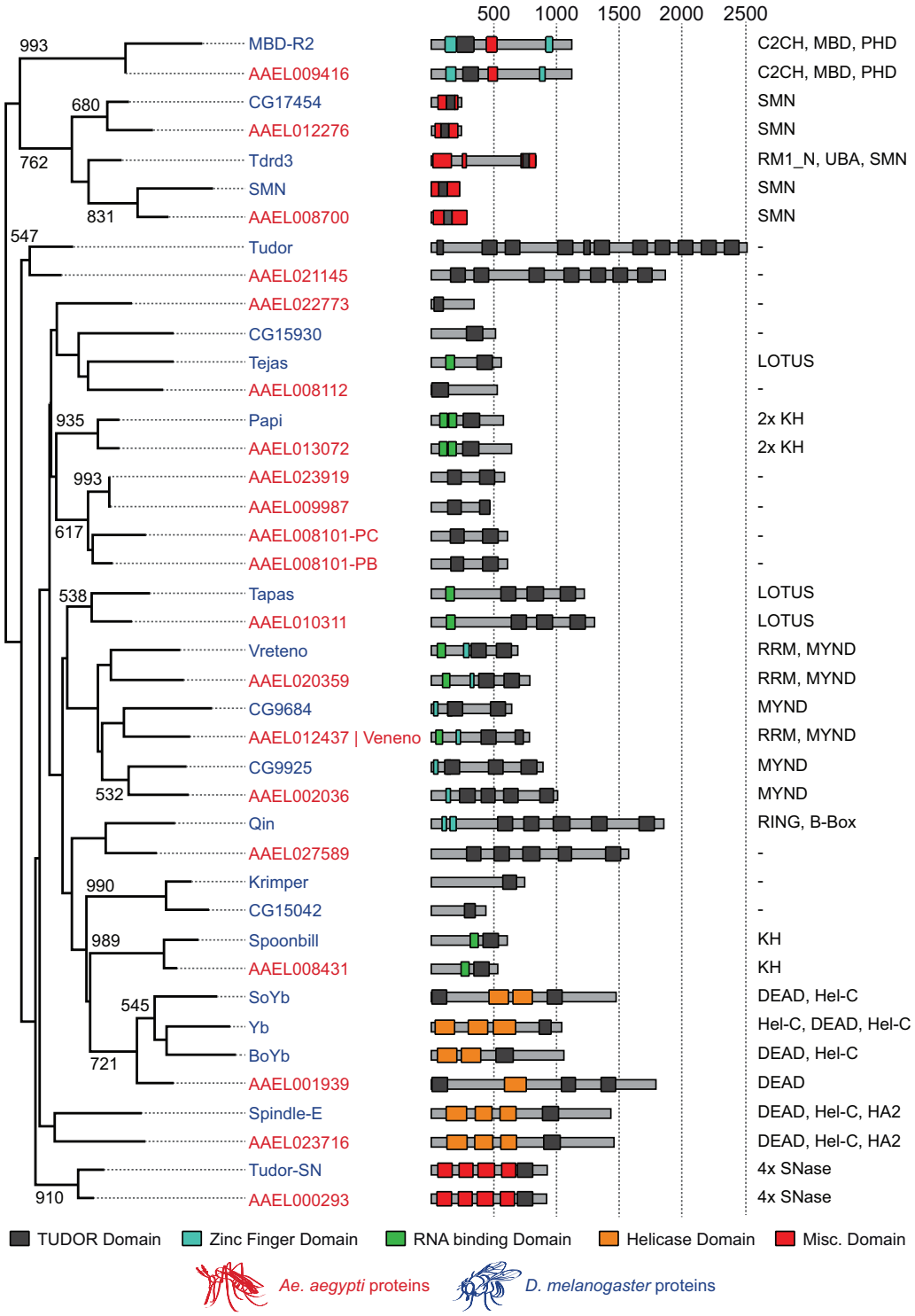

Figure 1. Orthologous Tudor genes in *Drosophila melanogaster* and *Aedes aegypti*. On the left, a neighbor joining tree based on TUDOR domains from *A. aegypti* (red) and *D. melanogaster* (blue) is shown. Numbers indicate bootstrap values for 1000 iterations; only values >500 are shown. In the middle, predicted domain structures of Tudor proteins are drawn schematically, with TUDOR domains shown in black, zinc fingers in blue, putative RNA binding domains in green, domains associated with helicase activity in orange and all other domains in red. Numbers at the top indicate protein length in amino acids. On the right, protein domains other than TUDOR domains are presented, ordered from amino to carboxyl terminus, as indicated in the middle panel. As the AAEL008101 gene produces two splice variants encoding TUDOR domains of slightly different composition (PB and PC), both were included as separate entities in the multiple sequence alignment. B-box, B-box type zinc finger (Zf) domain; C2CH, C2CH-type Zf domain; C2H2, C2H2-type Zf domain; DEAD, DEAD box domain; HA2, Helicase-associated domain; Hel-C, helicase C domain; KH, K homology RNA-binding domain; LOTUS, OST-HTH/LOTUS domain; MBD, Methyl-CpG-binding domain; MYND, MYND (myeloid, Nervy, DEAF-1)-type Zf domain; PHD, PHD-type Zf domain; RING, RING-type Zf domain; RMI1_N, RecQ mediated genome instability domain; RRM, RNA recognition motif; SMN, survival motor neuron domain; SNase, Staphylococcal nuclease homologue domain; UBA, ubiquitin associated domain.

where there is clear one-to-one orthology, *A. aegypti* genes will be named after their *Drosophila* ortholog throughout this study.

Aedes aegypti Tudor proteins are involved in vpiRNA biogenesis

We included all identified *A. aegypti* Tudor proteins along with AAEL004290 in a functional knockdown screen for vpiRNA biogenesis. AAEL004290 is the ortholog of Eggless, a histone methyltransferase involved in the piRNA pathway in *D. melanogaster* that is predicted to contain TUDOR domains (41,42), although it did not surface in our HHpred-based homology detection.

In a previous study, deep sequencing of small RNAs from SINV-infected Aag2 cells revealed that the majority of vpiRNAs are derived from an ∼200 nt hotspot in the SINV-capsid gene (Supplementary Figure S1A) (20). We selected four highly abundant sense (+) strand vpiRNA sequences from this hotspot region for small RNA northern blotting. Knockdown of the Tudor genes AAEL012437, Vreteno and SMN resulted in >3-fold reduction of vpiRNA levels in Aag2 cells, with knockdown of AAEL012437 resulting in the most prominent phenotype (Figure 2). Interestingly, knockdown of Qin resulted in a 3-fold increase in viral piRNA levels. Knockdown was generally efficient, resulting in a 50 to 80% reduction of mRNA abundance for most genes (Figure 2 and Supplementary Figure S1C). For genes with suboptimal knockdown efficiency (Yb, AAEL008101 and MBD-R2), we performed an additional knockdown experiment using different batches of dsRNA targeting these transcripts. Here, we found that vpiRNA levels are also diminished upon knockdown of Yb and AAEL008101-RB (Supplementary Figure S1B). The observed effect on vpiRNA levels cannot be explained by changes in viral replication, as only minor differences were seen in viral RNA levels across knockdowns under these experimental conditions (Figure 2 and Supplementary Figure S1B, D and E). Moreover, changes in vpiRNA production did not correlate with expression levels of capsid RNA, which is the source of vpiRNAs that we probed for in this screen ($R^2 = 0.0506$; Supplementary Figure S1F).

We have previously shown that biogenesis of genic piRNAs from histone H4 mRNA depends on amplification by Ago3 and Piwi5 (43). Interestingly, histone H4 mRNA-derived piRNA levels were not affected by AAEL012437 knockdown (Figure 2), whereas both histone H4 mRNA-derived piRNAs and vpiRNAs were strongly reduced by knockdown of AAEL008101-RB (Supplementary Figure S1B). These results suggest that Tudor proteins could mark piRISC complexes dedicated to specific classes of piRNAs and that AAEL012437 acts in a complex that preferentially processes piRNAs from viral transcripts. As depletion of AAEL012437 resulted in the most prominent reduction of vpiRNA levels in repeated experiments (Supplementary Figure S1G and H), we proceeded with a more detailed characterization of this protein. Since the word virus comes from the Latin translation of the noun 'poison', we named this Tudor protein after the indicative present of the Latin verb 'to poison': Veneno (Ven).

Depletion of Veneno predominantly affects production of viral piRNAs

Small RNA northern blotting is suitable for the detection of only a handful of highly abundant piRNAs. For a more comprehensive analysis of small RNA populations upon Ven knockdown (KD), we prepared small RNA deep sequencing libraries from Aag2 cells infected with SINV. Depletion of Ven resulted in a strong reduction of vpiRNA production from both strands (75% and 80% reduction of (+) and (−) strand-derived vpiRNAs, respectively), whereas viral siRNA levels were unaffected (Figure 3A and B). As reported previously (20), SINV-derived piRNAs exhibit the 1U/10A nucleotide bias and 5′ end overlap indicative of ping-pong dependent amplification (Figure 3C and D). The vpiRNAs that remain in dsVen libraries exhibit a less pronounced nucleotide bias (Supplementary Figure S2A) and 5′ end overlap (Figure 3D), indicating that ping-pong amplification is reduced upon Ven-KD. The distribution of piRNAs across the viral genome and their size profile is unchanged in Ven-KD libraries (Supplementary Figure S2B–E), indicating that Ven is not directly responsible for triggering vpiRNA production or determining vpiRNA length.

The effect of Ven-KD on piRNA production from transposable elements is relatively minor compared to the changes in vpiRNA production, especially for those derived from the (+) strand (25 and 55% reduction of piRNAs derived from (+) and (−) strand, respectively; Supplementary Figure S3A). As the vast majority (>75%) of all transposon-derived piRNAs in our libraries originate from Ty3-gypsy elements (Supplementary Figure S3B), the effects seen in this family may dominate the overall phenotype of transposon piRNAs. Indeed, stratification of transposon-derived piRNAs into subclasses reveals only a mild effect of Ven-KD on piRNA production from Ty3-gypsy elements, 15 and 55% reduction of (+) and (−) strand derived piRNAs, respectively (Figure 3A). The discrepancy between the effect of Ven-KD on vpiRNA production and Ty3-gypsy-derived piRNA production is especially intriguing as Ty3-gypsy elements comprise the only major class of transposable elements that is processed into piRNAs by the ping-pong amplification loop, as is evident from their strong ping-pong signature (Figure 3C and D; Supplementary Figure S3C). Depletion of Ven results in reduced levels BEL-Pao element-derived piRNAs from both strands (Figure 3A), which make up the second-largest group of transposon-derived piRNAs (Supplementary Figure S3B). In contrast to piRNAs derived from Ty3-gypsy elements, BEL-Pao piRNAs lack a 1U/10A nucleotide signature (Figure 3C) and display only a very minor 10 nt overlap of 5′ends (Figure 3D). Instead, both sense and antisense BEL-Pao-derived piRNAs are enriched for 1U, suggesting that their production does not depend on ping-pong amplification but rather on primary biogenesis or phased piRNA production. Generally, siRNA production was unchanged for all transposon subfamilies (Figure 3B and Supplementary Figure S3C). In accordance with northern blot analyses (Figure 2), ping-pong dependent histone H4 mRNA-derived piRNA levels were only mildly reduced upon Ven-KD (Figure 3A). Taken together, these findings suggest that

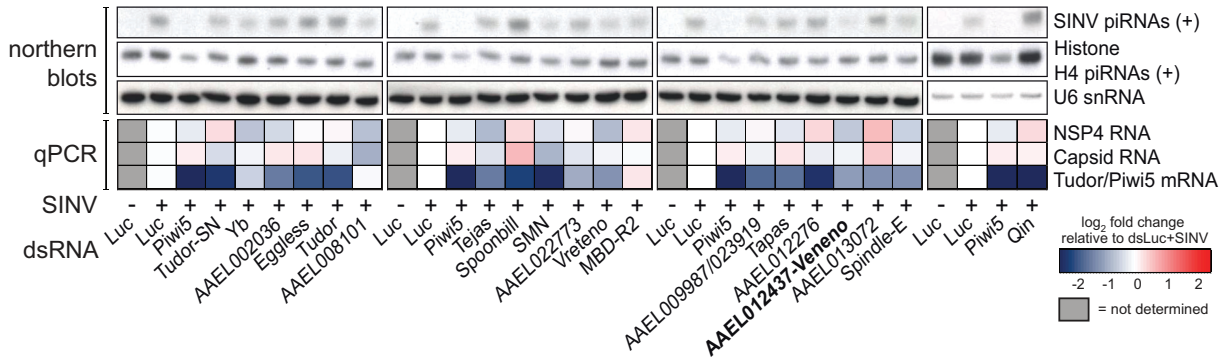

Figure 2. Loss of vpiRNA production upon knockdown of several Tudor genes. Tudor genes were knocked down in Aag2 cells by dsRNA transfection after which small RNA production of (+) strand SINV and histone H4 mRNA (H4)-derived piRNAs was assessed using northern blot analyses. dsRNA targeting luciferase (dsLuc) and Piwi5 were used as negative and positive controls, respectively. U6 snRNA was used as a loading control. *Aedes* proteins that have a clear one-to-one ortholog with similar domain composition are named after their *Drosophila* orthologs. The heat map depicts relative changes in NSP4 and Capsid viral RNA abundance and Tudor/Piwi5 knockdown efficiencies as determined by RT-qPCR. All expression values were normalized to SINV-infected dsLuc control samples. Gray boxes indicate samples for which no RT-qPCR was performed.

Ven supports ping-pong dependent piRNA biogenesis preferentially from viral RNA.

Veneno localizes to cytoplasmic foci

To further characterize the molecular function of Ven during vpiRNA biogenesis, we expressed GFP-tagged Ven and several domain mutants in Aag2 cells (Figure 4A). In the process of cloning these constructs, we noticed that the annotation of the Ven gene in AaegL3.5 on VectorBase was erroneous. We used Sanger sequencing of PCR products to revise the current gene annotation (Supplementary Figure S4), which was corroborated by published Aag2 transcriptome data and the recently released *Aedes aegypti* reference genome assembly AaegL5 (44,45). GFP-tagged Ven accumulated in cytoplasmic foci reminiscent of the piRNA processing granules *nuage* and Yb bodies in *D. melanogaster* (Figure 4B) (9,29). We tentatively term these foci Ven-bodies. In our revised annotation, Ven contains an RNA recognition motif (RRM) at its amino terminus. A mutant in which this motif has been removed (C91) retains its localization in Ven-bodies (Figure 4C), suggesting that putative RNA-binding by this domain is not required for granule formation. Additionally, Ven contains a Zn-finger of the MYND-type, a class of Zn-fingers predominantly involved in protein–protein interaction (46). Removal of this MYND-domain (C234) abolishes granular accumulation of Ven (Figure 4E and F). Intrinsically disordered sequences have recently been shown to mediate RNA binding and regulate RNA metabolism (47). Ven contains such an asparagine (N)-rich region directly upstream of the MYND-domain. A mutant in which this N-rich stretch and the RRM are removed (C199) but the MYND-domain is maintained, retains its localization in Ven-bodies (Figure 4D), which lends further support to the importance of the MYND-domain for the granular localization pattern.

Similarly, a glutamine (Q)-rich sequence directly downstream of the MYND-type Zn-finger is not sufficient for Ven-accumulation, as removal of the MYND domain alone (C234) disrupts Ven-body formation. Upon removal of the C-terminal (N670) or both TUDOR domains (N399), the distinct subcellular localization of Ven is largely retained, suggesting that TUDOR domains do not play a major role in granule formation (Figure 4G and H). To allow a more comprehensive analysis of Ven-body localization across mutants, we traced the cytoplasmic GFP-signal of ∼50 cells per transgene (as shown in Figure 4I) and quantified the coefficient of variance of this signal as a measure for granularity. This analysis confirms that Ven-body accumulation is abolished upon removal of the MYND-type Zn-finger. Also, a slight decrease in granularity is seen upon removal of either one (N670) or both (N399) TUDOR domains (Figure 4J), suggesting that additional protein-protein interactions may stabilize Ven-bodies. Altogether, these findings suggest that the MYND-type Zn-finger enables Ven localization into specific Ven-bodies where additional components of the mosquito piRNA machinery may be recruited for efficient piRNA production.

Veneno provides a molecular scaffold for a ping-pong amplification complex

Previously, we made use of epitope-tagged transgenes to show that the PIWI proteins Ago3 and Piwi5 are the core proteins that mediate ping-pong-dependent vpiRNA biogenesis in *A. aegypti* (20). Here, we use antibodies raised against endogenous PIWI proteins (Supplementary Figure S5A for antibody characterization) to confirm these findings. In accordance to our previous findings, sense strand-derived vpiRNAs are strongly enriched in Ago3-IP (Figure 5A), while antisense strand-derived vpiRNAs are enriched in Piwi5-IP (Figure 5B). Moreover, sense strand-derived vpiRNAs bound by Ago3 bear a strong 10A bias (Figure 5C, top panel), whereas antisense strand-derived vpiRNAs bound to Piwi5 have a 1U-bias (Figure 5D, bottom panel). Altogether, these data confirm that Ago3 and Piwi5 associate in a ping-pong amplification loop to produce vpiRNAs.

As Ven is important for efficient production of ping-pong dependent vpiRNAs (Figures 2–3), we hypothesized that the protein serves as a molecular scaffold to facilitate an interaction between the ping-pong partners Ago3 and Piwi5.

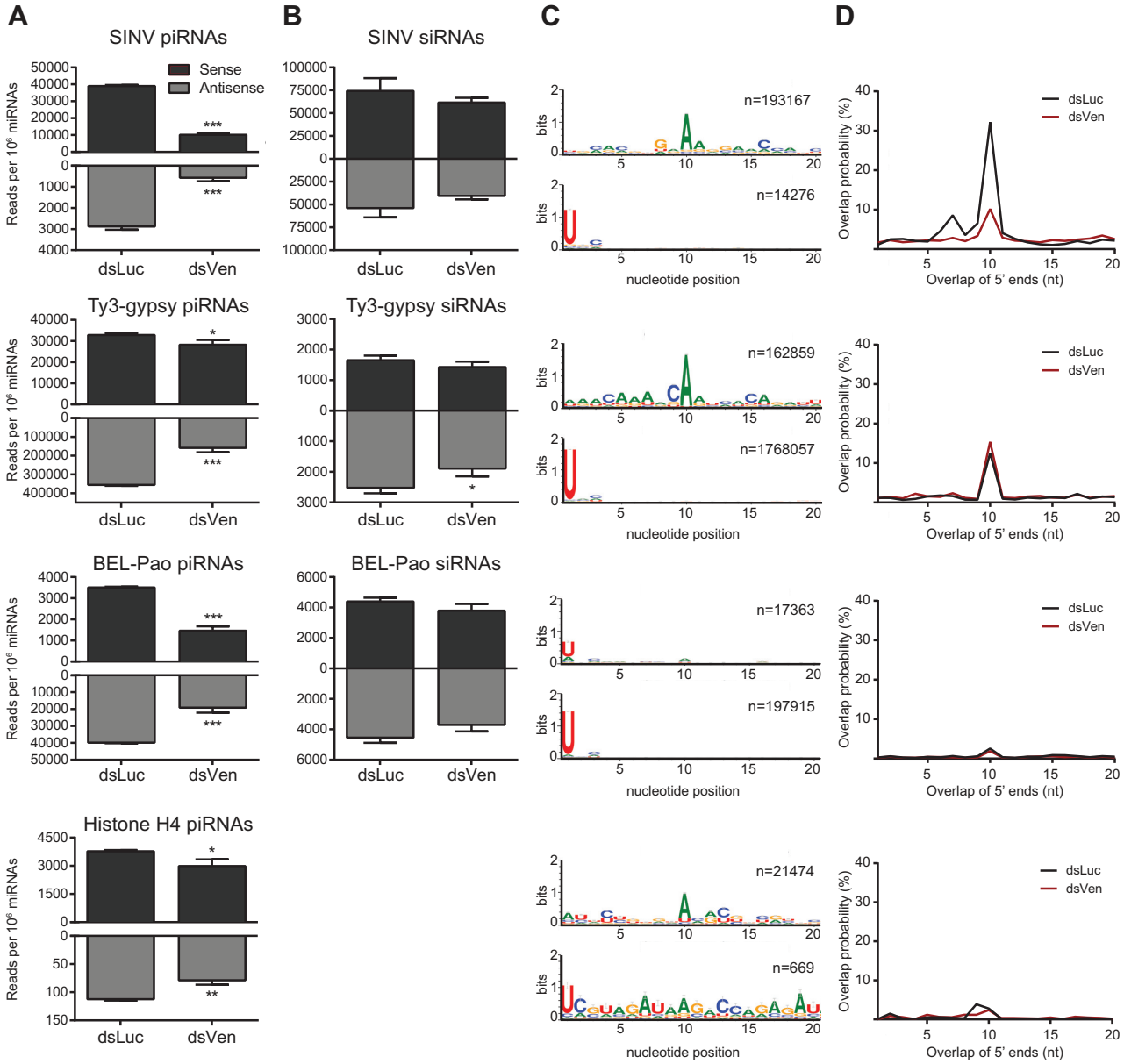

Figure 3. Veneno is required for efficient biogenesis of vpiRNAs. (**A** and **B**) Normalized read counts of 25–30 nt piRNAs (A) and 21 nt siRNAs (B) mapping to the SINV genome (top row), Ty3-gypsy transposons (second row), BEL-Pao transposons (third row) and histone H4 mRNA (bottom row) upon knockdown of Veneno (dsVen) and control knockdown (Firefly Luciferase, dsLuc). Virtually no siRNA-sized reads mapping to histone H4 mRNA were found (~200 reads per library), and these are therefore not shown. (**C**) Nucleotide bias at the first 20 positions of the 25–30 nt small RNA reads mapping to sense strand (upper panel) and antisense strand (lower panel) of the indicated RNA substrates in dsLuc libraries (n = number of reads). (**D**) The probability of 5′ overlap between piRNAs from opposite strands in dsLuc and dsVen libraries for the indicated classes of piRNAs. For bar charts in A and B, read counts of three independent libraries were normalized to the amount of miRNAs present in those libraries and analyzed separately for the sense (black) and antisense (gray) strands. Bars indicate mean ± standard deviation. Two-tailed student's t-test was used to determine statistical significance (*$P < 0.05$; **$P < 0.01$, ***$P < 0.001$). To generate sequence logos and 5′ overlap probability plots shown in C and D, reads of three independent libraries were combined.

To test this hypothesis, we immunoprecipitated GFP-tagged Ven and probed using antibodies recognizing endogenous Ago3 and Piwi5. We found that Ven interacts with Ago3, but not Piwi5, regardless of an ongoing SINV-infection (Figure 5E). IP of GFP alone does not copurify Ago3, confirming that the interaction is indeed mediated by Ven.

To further dissect the multimolecular network in which Ven participates, we employed quantitative MS of immunoprecipitated GFP-Ven complexes from both uninfected and SINV-infected Aag2 cells. These data confirm the association with Ago3 and reveal interesting additional Ven-interactors (Figure 5F and G; Supplementary Table S1). Specifically, Yb is enriched in Ven-complexes immunoprecipitated from both mock- and SINV-infected cells, which fits the observation that Yb knockdown reduces vpiRNA levels (Supplementary Figure S1B). Indeed, in small RNA

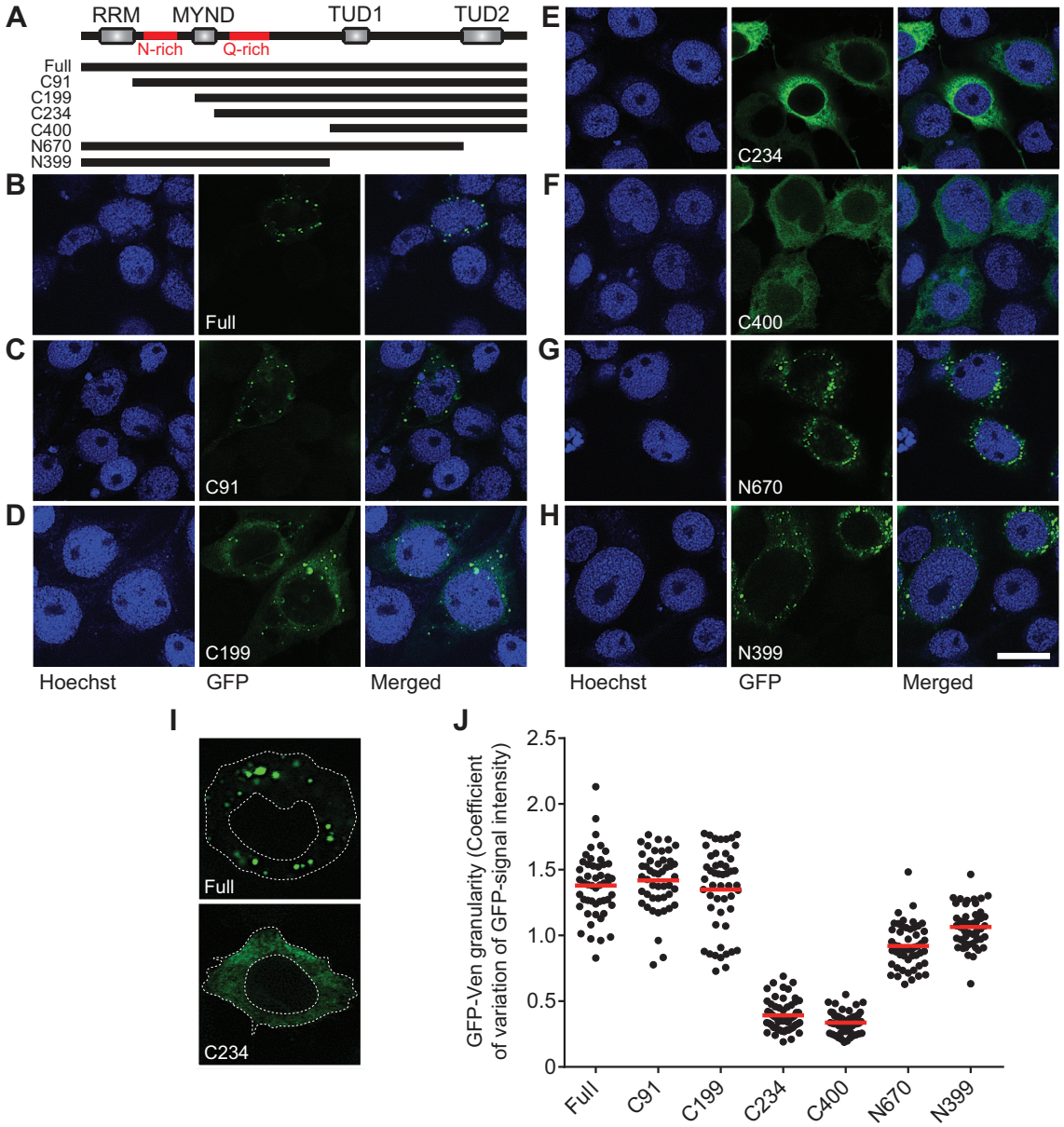

Figure 4. Veneno accumulates in cytoplasmic Ven-bodies. (**A**) Schematic representation of Ven transgenes used in IFA experiments. (Full: amino acid [aa] 1–785; C91: aa 91–785; C199: aa 199–785; C234: aa 234–785; C400: aa 400–785; N670: aa 1–670; N399: aa 1–399; red lines indicate sequences of low amino acid complexity, rich in asparagines [N] or glutamines [Q]). (**B**–**H**) Representative confocal images of Aag2 cells expressing transgenes drawn schematically in (A). Scale bar represents 10 μm. (**I**) The cytoplasm of 46–56 individual cells expressing GFP-tagged transgenes was traced as depicted and the mean and standard deviation of signal intensity was determined to calculate the coefficient of variation as a measure of signal granularity. (**J**) Scatter dot plot shows the GFP-signal granularity for individual cells; the red lines indicate the mean.

sequencing libraries, the effect of Yb-KD mirrors the effects seen in Ven-KD, with the strongest reduction in vpiRNA levels and only moderate effects on transposon- and histone H4 mRNA-derived piRNAs (Supplementary Figure S5E). The effects seen upon Yb-KD are less pronounced than those in Ven-KD libraries, which is likely due to relatively inefficient knockdown of Yb. Probing the Ven-interactome for orthologs of factors involved in the ping-pong amplification loop in *Drosophila*, we found a slight enrichment of AAEL004978, the *A. aegypti* ortholog of Vasa (Figure 5F and G). In *Drosophila*, Vasa recruits PIWI proteins to accommodate ping-pong amplification and is believed to be expressed exclusively in germline tissues. Yet, we verified that *A. aegypti* Vasa and other components of the piRNA biogenesis machinery are expressed in both germline and somatic tissues in female *A. aegypti* mosquitoes (Supplementary Figure S5B), implying that the complex is capable of producing vpiRNAs upon arbovirus infection in the soma.

We verified abovementioned interactions by co-purifying the constituents of the complex in reciprocal IPs followed by western blot (Figure 5H). Interestingly, we also detect

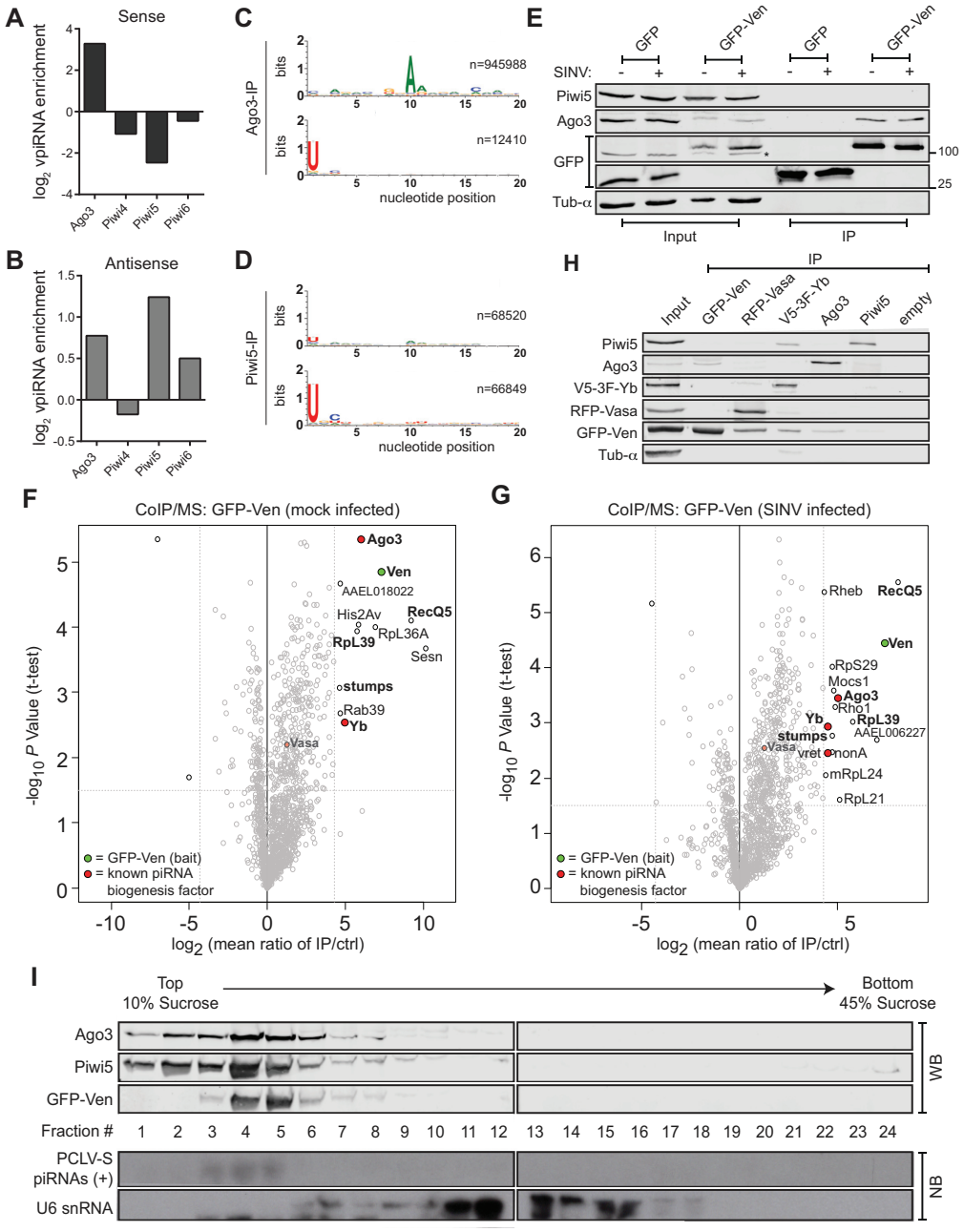

Figure 5. Characterization of a multi-protein complex containing the ping-pong partners Ago3 and Piwi5. (**A** and **B**) Enrichment of 25–30 nt small RNAs mapping to the SINV sense (A) and antisense (B) strand, relative to input, in small RNA sequencing libraries of IP of the indicated PIWI proteins. (**C** and **D**) Nucleotide bias at the first 20 positions of 25–30 nt small RNA reads mapping to sense strand (upper panel) and antisense strand (lower panel) in Ago3-IP (C) and Piwi5-IP (D) libraries. (**E**) Protein lysates from SINV-infected (+) and uninfected (−) Aag2 cells transfected with expression plasmids encoding GFP or GFP-Ven before (Input) and after GFP-IP were analyzed for (co)purification of endogenous Ago3 and Piwi5, as well as the GFP-tagged transgene by western blot. The asterisk indicates a non-specific band. (**F** and **G**) Identification of Ven-interacting proteins in lysates from both mock- (F) and SINV-infected Aag2 cells (G) by label-free quantitative (LFQ) MS. Permutation-based FDR-corrected *t*-tests were used to determine proteins that are statistically enriched in the Ven-IP. The LFQ-intensity of GFP-Ven IP over a control IP using the same lysate and non-specific beads (log_2-transformed) is plotted against the $-log_{10}$ *P*-value. Interactors with an enrichment of log_2 fold change > 4.3; $-log_{10}$ P value > 1.5 are indicated. Proteins in the top right corner represent the bait protein in green (Ven) and its interactors. Orthologs of known piRNA biogenesis factors in *Drosophila melanogaster* are indicated in red and interacting proteins present in both mock- and SINV-infected pulldowns are shown in bold font. Where available, interacting proteins were named according to their ortholog in *D. melanogaster*. In case of uncharacterized orthologous Drosophila proteins, we assigned the Vectorbase GeneID to the protein. (**H**) Reciprocal IPs of GFP-Ven, RFP-Vasa, V5-3xFlag-Yb, Ago3 and Piwi5 using antibodies targeting GFP, RFP, V5, Ago3 and Piwi5, respectively. Samples were probed with antibodies against GFP, RFP, Flag, Ago3, Piwi5 and α-tubulin, as indicated. (**I**) Lysate from Aag2 cells stably expressing GFP-Ven was fractionated on a 10–45% sucrose gradient. Protein fractions were size separated and stained using antibodies against GFP, Ago3 and Piwi5. RNA samples from those fractions were analyzed by northern blot analysis, using probes targeting abundant (+) strand ping-pong dependent piRNAs produced from the S-segment of the bunyavirus Phasi Charoen-like virus (PCLV) and U6 snRNA. All fractions contain proteinaceous material as is evidenced by silver staining (Supplementary Figure S5C); spliceosomal ribonucleoprotein complexes are enriched in fractions 11–16, as evidenced by the presence of U6 snRNA.

Piwi5 as a direct interaction partner of Yb (Figure 5H). In sucrose density gradient fractionation, Ven co-sediments with Ago3 and Piwi5 (most prominently in fractions 4–5) and with piRNAs produced from the S-segment of the Phasi Charoen-like bunyavirus (Figure 5I), a known contaminant of the Aag2 cell line which has previously been reported to produce piRNAs through ping-pong amplification (48,49). Altogether, this further suggests that Ven forms a multi-protein complex with Ago3 and Piwi5. In accordance, we find that Ven, Ago3, Piwi5, Yb and Vasa colocalize in Ven bodies, suggesting that these granules are indeed the sites of vpiRNA biogenesis (Supplementary Figure S5D). Together, these findings define a multi-molecular complex in which the ping-pong partners Ago3 and Piwi5 are brought together by the Tudor proteins Ven and Yb to promote efficient piRNA production (Figure 6F).

Ven-Ago3 interaction depends on sDMA-recognition

Interaction between Tudor and PIWI proteins generally depends on recognition of sDMAs on PIWI proteins by an aromatic cage in the TUDOR domain (25). To further characterize the domain required for the interaction between Ven and Ago3, we immunoprecipitated truncated Ven transgenes and assessed copurification of Ago3. A truncated Ven-mutant lacking the RRM (C206, Figure 6A) still strongly associates with Ago3 (Figure 6C). Moreover, this mutant retains its association in a complex involving Yb, Vasa and Piwi5 as shown by MS (Supplementary Figure S6A, Supplementary Table S2) and reciprocal IPs (Supplementary Figure S6B). The MYND-domain mutant (C234), in which the distinct localization pattern is distorted (Figure 4), still aptly binds Ago3, suggesting that granular localization in Ven-bodies is not required for Ago3-interaction (Figure 6C). The carboxyl terminus containing two TUDOR domains (C400) is sufficient for interaction with Ago3, whereas Ago3-binding is lost upon deletion of the second (206-669) or both (206-399) TUDOR domains (Figure 6C). However, this loss of binding may result from reduced expression or stability of these mutants.

To further specify whether Ven-Ago3 interaction is TU DOR domain mediated, we generated Ven transgenes carrying point mutations in residues predicted to be involved in sDMA recognition (2Δ: C206-G463A/Y465A and 4Δ: C206-G463A/Y465A/D483A/N486A; Figure 6B). We found that the second TUDOR domain of Ven is atypical in that only one of the predicted aromatic cage residues is conserved (Supplementary Figure S6C). We therefore analyzed binding of Ago3 to Ven that carries point mutations in the first TUDOR domain. Interaction with Ago3 was lost in these mutants, suggesting that the first TUDOR domain of Ven binds Ago3 in a canonical sDMA-dependent manner (Figure 6C). It is likely that the C-terminal TUDOR domain is not involved in Ago3 binding via sDMAs since critical residues are not conserved (Supplementary Figure S6C). However, we cannot fully exclude that cooperative binding of both TUDOR domains by Ago3 is required for efficient association with Ven. To verify that Ago3 bears sDMA modifications, we made use of Aag2 cells stably expressing GFP-tagged Ago3 to enable simultaneous detection of GFP-Ago3 and sDMA modifications. We found a specific sDMA signal overlapping with the signal of immunopurified GFP-Ago3 (Figure 6D), indicating that Ago3 indeed contains sDMAs. Endogenous Ago3 present in Ven-complexes also bears sDMAs, further supporting the notion that Ven-Ago3 interaction is mediated by sDMA recognition. The interaction with Ago3 is not required for localization of Ven in Ven-bodies, as introducing the indicated point mutations (G463A/Y465A) in the context of the full length protein does not affect its subcellular localization pattern (Figure 6E). Altogether, our findings support a model in which Veneno, through sDMA recognition, recruits Ago3 to a multi-molecular complex that promotes ping-pong amplification of piRNAs preferentially from exogenous RNAs (Figure 6F).

DISCUSSION

Mosquito antiviral immunity largely relies on the processing of viral dsRNA into virus-derived siRNAs that direct the degradation of viral RNA. Processing of viral dsRNA into vsiRNAs by the siRNA pathway has been thoroughly characterized in mosquitoes (50,51). The discovery of *de novo* production of vpiRNAs from arboviral RNA however, uncovered the intriguing possibility of an additional small RNA-based line of defense against arboviruses. We previously reported that, in *A. aegypti*, vpiRNAs are amplified by the ping-pong partners Ago3 and Piwi5 (20). However, these conclusions were based on experiments in which transgenic constructs were used. As transient expression of transgenic constructs poses the risk of expression at non-physiological levels, we used antibodies raised against endogenous PIWI-proteins in this study to confirm that Ago3 and Piwi5 indeed associate in a ping-pong amplification loop that produces vpiRNAs. Moreover, as observed before, we find that Piwi4 is depleted of viral piRNAs. As of yet, it is unclear how viral RNA produced in the cytoplasm is entered into the piRNA pathway, especially as canonical substrates for the piRNA pathway are genomically encoded single-stranded precursors (3,4). To better understand how viral RNA is detected by the somatic piRNA pathway of mosquitoes, we have defined the molecular machinery that processes viral RNA into vpiRNAs. Our results support a model in which the Tudor protein Veneno recruits Yb, Piwi5 and Ago3 to perinuclear foci to assemble a multi-protein complex for efficient ping-pong-dependent piRNA production from exogenous viral RNA.

Multiple Tudor proteins are required for viral piRNA biogenesis

As a tightly regulated network of Tudor proteins promotes production of piRNAs in *Drosophila* (21,22), we performed a comprehensive knockdown screen to evaluate the role of *A. aegypti* Tudor proteins in vpiRNA biogenesis. Knockdown of several Tudor genes affects vpiRNA biogenesis, with knockdown of Veneno (Ven) resulting in the strongest depletion of vpiRNAs. Thus far, the direct ortholog of Ven in *D. melanogaster* (CG9684) has not been studied extensively. In a systematic analysis of all *Drosophila* Tudor proteins, germline-specific knockdown of CG9684 did not affect steady-state levels of transposon transcripts or female

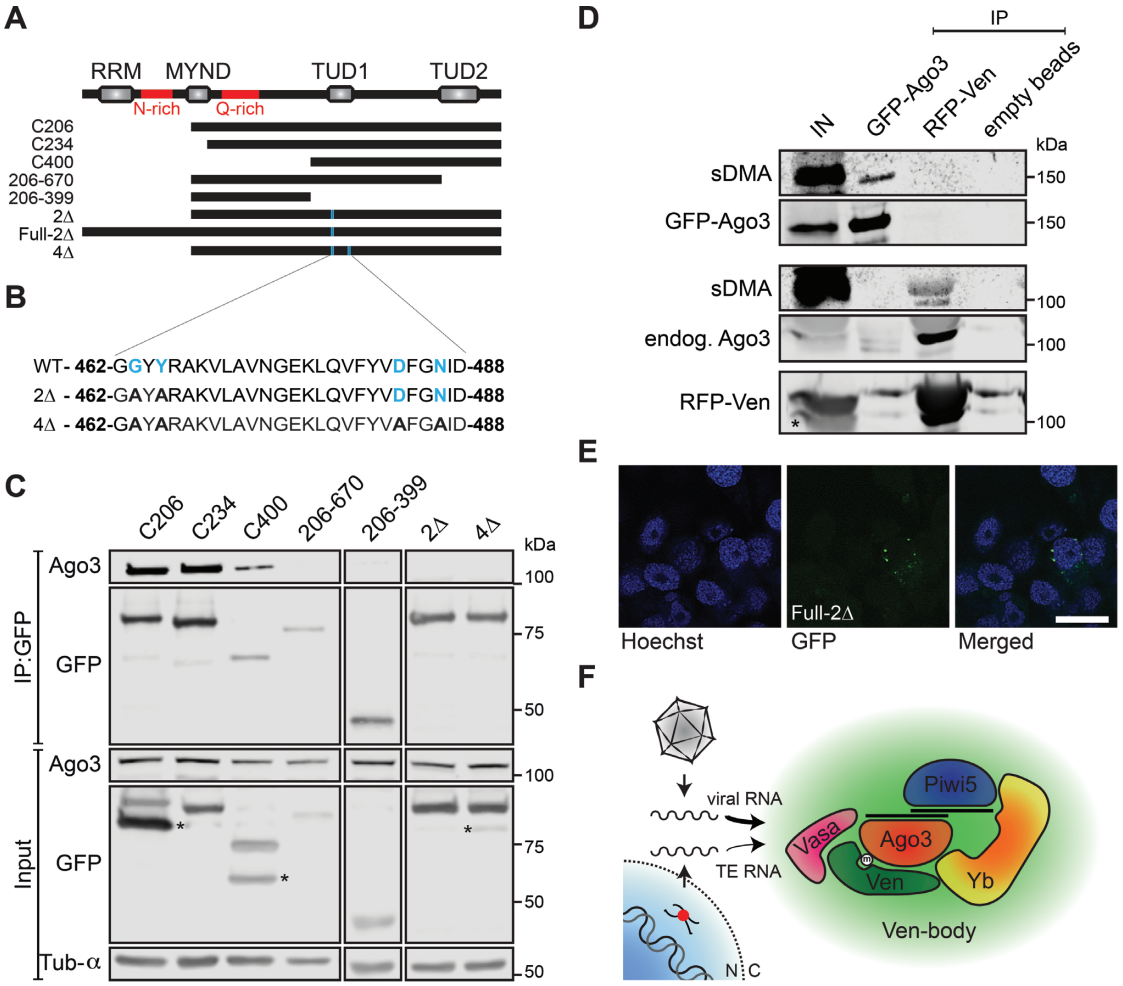

Figure 6. Ven-Ago3 interaction is mediated by sDMA-recognition. (**A**) Schematic representation of Veneno transgenes used in Ago3 co-IP experiments. (C206: amino acid [aa] 206–785; C234: aa 234–785; C400: aa 400–785; 206–669: aa 206–669; 206–399: aa 206–399; 2Δ: C206-G463A/Y465A; Full-2Δ: G463A/Y465A; 4Δ: C206-G463A/Y465A/D483A/N486A; red lines indicate sequences of low amino acid complexity, rich in asparagines [N] or glutamines [Q]). (**B**) Sequence corresponding to a part of the first TUDOR domain with residues indicated that were mutated in the 2Δ and 4Δ transgenes. Residues indicated in blue bold font are predicted to be involved in sDMA recognition. (**C**) Lysates from Aag2 cells expressing the indicated GFP-tagged Ven transgenes were subjected to GFP-IP and subsequently analyzed for co-purification of Ago3 by western blot. α-Tubulin serves as loading control. Asterisks indicate non-specific bands. (**D**) Lysate from Aag2 cells stably expressing GFP-Ago3 and transiently transfected with a plasmid encoding RFP-Ven was immunoprecipitated using GFP-, RFP- and empty beads. Western blots were stained using antibodies for GFP, RFP and symmetrical dimethylated arginines (sDMA). The asterisk indicates a non-specific band. (**E**) Representative confocal image of Aag2 cells expressing GFP-tagged Ven-2Δ-mutant; scale bar represents 10 μm. (**F**) Schematic model of the identified multi-protein complex responsible for ping-pong amplification of exogenous (viral) and endogenous (transposable element, TE)-derived piRNAs. The thickness of the arrows reflects the relative contribution of the complex to processing of different RNA substrates. N, nucleus; C, cytoplasm.

fertility rate (28). This study, however, did not evaluate the effect of CG9684 knockdown on small RNA populations, raising the possibility that CG9684 is involved in biogenesis of non-transposon-derived piRNAs.

Additional Tudor proteins that are involved in vpiRNA production are Yb and AAEL008101-RB, a gene that lacks a one-to-one ortholog in the fruit fly. Whereas involvement of Yb in vpiRNA biogenesis can be explained by its central place in the multi-protein complex discovered in this study, the molecular function of AAEL008101-RB remains to be elucidated. We cannot exclude that additional Tudor proteins play a role in vpiRNA biogenesis, which may be masked by redundancy of paralogous proteins or residual protein activity after suboptimal knockdown efficiency.

piRNA production occurs in discrete cytoplasmic foci

Ven accumulates in cytoplasmic foci similar to piRNA processing bodies in the fly. In *Drosophila* somatic follicle cells, which surround the germ cells, primary piRNA biogenesis takes place in Yb bodies. One of the core factors present in these structures is their eponym Yb (28–30). Yet, no piRNA amplification takes place in Yb bodies, since the ping-pong partners Aub and Ago3 are not expressed in follicle cells (52,53). In contrast, in *Drosophila* germ cells piRNA amplification takes place in the *nuage* and one of the core proteins of this perinuclear structure is the helicase Vasa (9,26,27). In *Drosophila* and the silkworm *Bombyx mori*, Vasa is directly implicated in secondary piRNA amplification by preventing non-specific degradation of piRNA precursors and

facilitating their transfer to PIWI proteins (26). Yb is not present in *nuage*, but it has been suggested that its function may be taken over by its paralogous family members: brother and sister of Yb (BoYb and SoYb, respectively) (28). *A. aegypti* encodes only a single paralog of Yb, which associates directly with Ven and Piwi5 and is required for efficient vpiRNA biogenesis. The presence of a multi-protein complex containing orthologs of Vasa and Yb supports the idea that Ven-bodies resemble *nuage*-like piRNA processing bodies.

Both in *A. aegypti* and *D. melanogaster*, ping-pong dependent piRNA biogenesis depends on Tudor proteins recruiting PIWI proteins to perinuclear granules. Yet, whereas the biogenesis machinery in both insects adheres to the same principles, the mechanisms that assemble the ping-pong amplification complex in these granules differ substantially. In *Drosophila*, the Tudor protein Krimper interacts directly with both partners in the ping-pong loop (Ago3 and Aub) and recruits them to the *nuage* (54,55). In *A. aegypti*, Ven associates directly with Ago3 and recruits Piwi5 via another Tudor protein (Yb) to Ven-bodies. Additionally, whereas sDMA modifications are dispensable for Krimper-Ago3 interaction, Ven binds Ago3 in an sDMA-dependent manner in *A. aegypti*. Lastly, while the ping-pong amplification machinery is specific to the germline in *D. melanogaster*, the proteins involved in the multi-protein complex described in this study are expressed ubiquitously in *A. aegypti*.

Production of piRNAs from exogenous and endogenous sources

Knockdown of Ven greatly affects production of piRNAs derived from exogenous viral RNA, while only a modest reduction is seen for genic histone H4 mRNA- and transposon-derived secondary piRNA levels. The apparent stability of histone H4 mRNA-derived piRNAs is especially surprising, as their production has previously been shown to depend on ping-pong amplification involving the PIWI proteins Ago3 and Piwi5 (43). Similarly, ping-pong dependent piRNA production from Ty3-gypsy transposable elements is affected only mildly by Ven-KD. The apparent preference of Ven for virus-derived piRNAs is markedly different from the Tudor protein AAEL008101-RB, which is required for efficient biogenesis of both virus- and histone H4 mRNA-derived piRNAs. Yet, we cannot formally exclude that the experimental set-up may partially explain the stronger effect of Ven-KD on vpiRNAs. As piRNAs were analyzed upon acute viral infection, vpiRNA are produced *de novo* under Ven-KD conditions. This is in contrast to endogenous piRNAs and their precursors (piRNA cluster transcripts, mRNAs), which are pre-existent prior to the establishment of Ven-KD. Hence, *de novo* vpiRNA production may be especially sensitive to perturbed Ven expression.

Bel-Pao-derived piRNA production is largely independent of ping-pong amplification, as is evident from the weak 1U/10A signature and 10 nt overlap of piRNA 5′ends. Therefore, we were surprised to find a strong reduction in Bel-Pao-derived piRNAs upon Ven-KD. Apart from secondary piRNA production in the ping-pong loop, piRNA-mediated cleavage of transposon mRNA may trigger the production of phased piRNAs bearing a strong 1U bias (10,11). This mechanism of phased piRNA production seems to be particularly active in *A. aegypti* (56). Hence, a modest reduction of ping-pong-dependent piRNA levels may result in strong reduction of phased piRNA production which could explain the strong effect of Ven-KD of production of BEL-Pao-derived piRNAs.

Our data suggest that Ven is involved in specifying the substrate for piRNA production and may preferentially shuttle viral RNA into the ping-pong loop. It would be interesting to assess whether viral RNA from other arbovirus families are similarly affected by Ven knockdown, which would point toward a more general role of Ven in self-nonself discrimination, a hallmark of an effective immune response. Dependency on specific co-factors for the biogenesis of small RNAs from different RNA sources is not unprecedented. For example, the siRNA pathway co-factor Loqs-PD is required for processing of endogenous siRNA-precursors, but is dispensable for siRNA production from exogenous dsRNA or viral RNA (57,58). Another study showed that the Tudor protein Qin/Kumo specifically prevents (+) strand transposon RNAs from becoming Piwi-bound piRNAs during the process of piRNA phasing (59). Analogies can also be drawn to the vertebrate piRNA pathway, where Tdrd1, the closest mouse ortholog of Ven, ensures processing of the correct transcripts by the piRNA pathway (60). Accordingly, the PIWI protein Mili contains a disproportionally large population of piRNAs derived from cellular mRNA and ribosomal RNA in *Tdrd1* knockout mice. In a similar fashion, Ven could promote processing specifically of viral RNA by the mosquito piRNA pathway. Yet, we expect the molecular mechanism underlying this Tudor protein-guided sorting to be different as Tdrd1 interacts with Mili, the PIWI protein that predominantly binds 1U biased primary piRNAs, whereas Ven associates with Ago3, which mainly binds 10A biased secondary piRNAs.

A sophisticated network of accessory proteins that guides diverse RNA substrates into distinct piRISC complexes may be of particular importance in *A. aegypti* as this mosquito species encodes an expanded PIWI gene family consisting of seven members (61,62), of which four (*Ago3* and *Piwi 4–6*) are expressed in somatic tissues (63). Moreover, the repertoire of RNA molecules that are processed into piRNAs is extended to include viral RNA (13). Tudor proteins like Veneno may therefore aid in streamlining piRNA processing and allow flexible adaptation of the piRNA pathway in response to internal and external stimuli such as arbovirus infection.

DATA AVAILABILITY

Small RNA sequencing data have been deposited in the NCBI sequence read archive under SRA accession SRP127210. The MS proteomics data have been deposited to the ProteomeXchange Consortium via the PRIDE partner repository with the dataset identifier PXD009997.

SUPPLEMENTARY DATA

Supplementary Data are available at NAR Online.

ACKNOWLEDGEMENTS

We thank members of the Van Rij laboratory for fruitful discussions, Eugene Berezikov (European Research Institute for the Biology of Aging) for bioinformatic advice, the Microscopic Imaging Centre of Radboudumc for support for confocal microscopy, and Siebe van Genesen for assistance with density gradient fractionation. Sequencing was performed by the GenomEast platform, a member of the 'France Génomique' consortium (ANR-10-INBS-0009). We would also like to thank Gorben Pijlman (University of Wageningen) for kindly providing the pPUbB-GW vector, Frank van Kuppeveld (Utrecht University) for the rabbit-anti-GFP antibody, and the Carnegie Institution of Washington for the Drosophila Gateway Vector collection.

FUNDING

Radboud University Medical Center PhD Fellowship (to P.M.); European Research Council (ERC) Consolidator Grant under the European Union's Seventh Framework Programme [ERC CoG 615680 to R.P.vR.]; Netherlands Organization for scientific Research, VICI Grant [016.VICI.170.090 to R.P.vR.]; Dutch Cancer Society, The Oncode Institute (to M.V.).Funding for open access charge: ERC [ERC CoG 615680].

Conflict of interest statement. None declared.

REFERENCES

1. Ghildiyal,M. and Zamore,P.D. (2009) Small silencing RNAs: an expanding universe. *Nat. Rev. Genet.*, **10**, 94–108.
2. Meister,G. (2013) Argonaute proteins: functional insights and emerging roles. *Nat. Rev. Genet.*, **14**, 447–459.
3. Czech,B. and Hannon,G.J. (2016) One loop to rule them All: The Ping-Pong cycle and piRNA-guided silencing. *Trends Biochem. Sci.*, **41**, 324–337.
4. Hirakata,S. and Siomi,M.C. (2016) piRNA biogenesis in the germline: from transcription of piRNA genomic sources to piRNA maturation. *Biochim. Biophys. Acta*, **1859**, 82–92.
5. Lim,R.S. and Kai,T. (2015) A piece of the pi(e): the diverse roles of animal piRNAs and their PIWI partners. *Semin. Cell Dev. Biol.*, **47–48**, 17–31.
6. Brennecke,J., Aravin,A.A., Stark,A., Dus,M., Kellis,M., Sachidanandam,R. and Hannon,G.J. (2007) Discrete small RNA-generating loci as master regulators of transposon activity in Drosophila. *Cell*, **128**, 1089–1103.
7. Gunawardane,L.S., Saito,K., Nishida,K.M., Miyoshi,K., Kawamura,Y., Nagami,T., Siomi,H. and Siomi,M.C. (2007) A slicer-mediated mechanism for repeat-associated siRNA 5′ end formation in Drosophila. *Science*, **315**, 1587–1590.
8. Cora,E., Pandey,R.R., Xiol,J., Taylor,J., Sachidanandam,R., McCarthy,A.A. and Pillai,R.S. (2014) The MID-PIWI module of Piwi proteins specifies nucleotide- and strand-biases of piRNAs. *RNA*, **20**, 773–781.
9. Lim,A.K. and Kai,T. (2007) Unique germ-line organelle, nuage, functions to repress selfish genetic elements in Drosophila melanogaster. *PNAS*, **104**, 6714–6719.
10. Mohn,F., Handler,D. and Brennecke,J. (2015) Noncoding RNA. piRNA-guided slicing specifies transcripts for Zucchini-dependent, phased piRNA biogenesis. *Science*, **348**, 812–817.
11. Han,B.W., Wang,W., Li,C., Weng,Z. and Zamore,P.D. (2015) Noncoding RNA. piRNA-guided transposon cleavage initiates Zucchini-dependent, phased piRNA production. *Science*, **348**, 817–821.
12. Lewis,S.H., Quarles,K.A., Yang,Y., Tanguy,M., Frezal,L., Smith,S.A., Sharma,P.P., Cordaux,R., Gilbert,C., Giraud,I. *et al.* (2018) Pan-arthropod analysis reveals somatic piRNAs as an ancestral defence against transposable elements. *Nat. Ecol. Evolu.*, **2**, 174–181.
13. Miesen,P., Joosten,J. and van Rij,R.P. (2016) PIWIs Go Viral: Arbovirus-derived piRNAs in vector mosquitoes. *PLoS Pathog.*, **12**, e1006017.
14. Kraemer,M.U., Sinka,M.E., Duda,K.A., Mylne,A.Q., Shearer,F.M., Barker,C.M., Moore,C.G., Carvalho,R.G., Coelho,G.E., Van Bortel,W. *et al.* (2015) The global distribution of the arbovirus vectors Aedes aegypti and Ae. albopictus. *Elife*, **4**, e08347.
15. Lambrechts,L. and Scott,T.W. (2009) Mode of transmission and the evolution of arbovirus virulence in mosquito vectors. *Proc. Biol. Sci.*, **276**, 1369–1378.
16. Myles,K.M., Wiley,M.R., Morazzani,E.M. and Adelman,Z.N. (2008) Alphavirus-derived small RNAs modulate pathogenesis in disease vector mosquitoes. *PNAS*, **105**, 19938–19943.
17. Samuel,G.H., Wiley,M.R., Badawi,A., Adelman,Z.N. and Myles,K.M. (2016) Yellow fever virus capsid protein is a potent suppressor of RNA silencing that binds double-stranded RNA. *PNAS*, **113**, 13863–13868.
18. Sanchez-Vargas,I., Scott,J.C., Poole-Smith,B.K., Franz,A.W., Barbosa-Solomieu,V., Wilusz,J., Olson,K.E. and Blair,C.D. (2009) Dengue virus type 2 infections of Aedes aegypti are modulated by the mosquito's RNA interference pathway. *PLoS Pathog.*, **5**, e1000299.
19. Cirimotich,C.M., Scott,J.C., Phillips,A.T., Geiss,B.J. and Olson,K.E. (2009) Suppression of RNA interference increases alphavirus replication and virus-associated mortality in Aedes aegypti mosquitoes. *BMC Microbiol.*, **9**, 49.
20. Miesen,P., Girardi,E. and van Rij,R.P. (2015) Distinct sets of PIWI proteins produce arbovirus and transposon-derived piRNAs in Aedes aegypti mosquito cells. *Nucleic Acids Res.*, **43**, 6545–6556.
21. Siomi,M.C., Mannen,T. and Siomi,H. (2010) How does the royal family of Tudor rule the PIWI-interacting RNA pathway? *Genes Dev.*, **24**, 636–646.
22. Pek,J.W., Anand,A. and Kai,T. (2012) Tudor domain proteins in development. *Development*, **139**, 2255–2266.
23. Maurer-Stroh,S., Dickens,N.J., Hughes-Davies,L., Kouzarides,T., Eisenhaber,F. and Ponting,C.P. (2003) The tudor domain 'Royal Family': Tudor, plant agenet, chromo, PWWP and MBT domains. *Trends Biochem. Sci.*, **28**, 69–74.
24. Kirino,Y., Kim,N., de Planell-Saguer,M., Khandros,E., Chiorean,S., Klein,P.S., Rigoutsos,I., Jongens,T.A. and Mourelatos,Z. (2009) Arginine methylation of Piwi proteins catalysed by dPRMT5 is required for Ago3 and Aub stability. *Nat. Cell Biol.*, **11**, 652–658.
25. Liu,H., Wang,J.Y., Huang,Y., Li,Z., Gong,W., Lehmann,R. and Xu,R.M. (2010) Structural basis for methylarginine-dependent recognition of Aubergine by Tudor. *Genes Dev.*, **24**, 1876–1881.
26. Xiol,J., Spinelli,P., Laussmann,M.A., Homolka,D., Yang,Z., Cora,E., Coute,Y., Conn,S., Kadlec,J., Sachidanandam,R. *et al.* (2014) RNA clamping by Vasa assembles a piRNA amplifier complex on transposon transcripts. *Cell*, **157**, 1698–1711.
27. Patil,V.S. and Kai,T. (2010) Repression of retroelements in Drosophila germline via piRNA pathway by the Tudor domain protein Tejas. *Curr. Biol.*, **20**, 724–730.
28. Handler,D., Olivieri,D., Novatchkova,M., Gruber,F.S., Meixner,K., Mechtler,K., Stark,A., Sachidanandam,R. and Brennecke,J. (2011) A systematic analysis of Drosophila TUDOR domain-containing proteins identifies Vreteno and the Tdrd12 family as essential primary piRNA pathway factors. *EMBO J.*, **30**, 3977–3993.
29. Saito,K., Ishizu,H., Komai,M., Kotani,H., Kawamura,Y., Nishida,K.M., Siomi,H. and Siomi,M.C. (2010) Roles for the Yb body components Armitage and Yb in primary piRNA biogenesis in Drosophila. *Genes Dev.*, **24**, 2493–2498.
30. Olivieri,D., Sykora,M.M., Sachidanandam,R., Mechtler,K. and Brennecke,J. (2010) An in vivo RNAi assay identifies major genetic and cellular requirements for primary piRNA biogenesis in Drosophila. *EMBO J.*, **29**, 3301–3317.
31. Zamparini,A.L., Davis,M.Y., Malone,C.D., Vieira,E., Zavadil,J., Sachidanandam,R., Hannon,G.J. and Lehmann,R. (2011) Vreteno, a gonad-specific protein, is essential for germline development and primary piRNA biogenesis in Drosophila. *Development*, **138**, 4039–4050.

32. Soding,J., Biegert,A. and Lupas,A.N. (2005) The HHpred interactive server for protein homology detection and structure prediction. *Nucleic Acids Res.*, **33**, W244–W248.
33. Finn,R.D., Clements,J., Arndt,W., Miller,B.L., Wheeler,T.J., Schreiber,F., Bateman,A. and Eddy,S.R. (2015) HMMER web server: 2015 update. *Nucleic Acids Res.*, **43**, W30–W38.
34. Di Tommaso,P., Moretti,S., Xenarios,I., Orobitg,M., Montanyola,A., Chang,J.M., Taly,J.F. and Notredame,C. (2011) T-Coffee: a web server for the multiple sequence alignment of protein and RNA sequences using structural information and homology extension. *Nucleic Acids Res.*, **39**, W13–W17.
35. Hahn,C.S., Hahn,Y.S., Braciale,T.J. and Rice,C.M. (1992) Infectious Sindbis virus transient expression vectors for studying antigen processing and presentation. *PNAS*, **89**, 2679–2683.
36. Saleh,M.C., Tassetto,M., van Rij,R.P., Goic,B., Gausson,V., Berry,B., Jacquier,C., Antoniewski,C. and Andino,R. (2009) Antiviral immunity in Drosophila requires systemic RNA interference spread. *Nature*, **458**, 346–350.
37. Pall,G.S. and Hamilton,A.J. (2008) Improved northern blot method for enhanced detection of small RNA. *Nat. Protoc.*, **3**, 1077–1084.
38. van Cleef,K.W., van Mierlo,J.T., Miesen,P., Overheul,G.J., Fros,J.J., Schuster,S., Marklewitz,M., Pijlman,G.P., Junglen,S. and van Rij,R.P. (2014) Mosquito and Drosophila entomobirnaviruses suppress dsRNA- and siRNA-induced RNAi. *Nucleic Acids Res.*, **42**, 8732–8744.
39. Smits,A.H., Jansen,P.W., Poser,I., Hyman,A.A. and Vermeulen,M. (2013) Stoichiometry of chromatin-associated protein complexes revealed by label-free quantitative mass spectrometry-based proteomics. *Nucleic Acids Res.*, **41**, e28.
40. Rappsilber,J., Mann,M. and Ishihama,Y. (2007) Protocol for micro-purification, enrichment, pre-fractionation and storage of peptides for proteomics using StageTips. *Nat. Protoc.*, **2**, 1896–1906.
41. Ishizu,H., Siomi,H. and Siomi,M.C. (2012) Biology of PIWI-interacting RNAs: new insights into biogenesis and function inside and outside of germlines. *Genes Dev.*, **26**, 2361–2373.
42. Clough,E., Moon,W., Wang,S., Smith,K. and Hazelrigg,T. (2007) Histone methylation is required for oogenesis in Drosophila. *Development*, **134**, 157–165.
43. Girardi,E., Miesen,P., Pennings,B., Frangeul,L., Saleh,M.C. and van Rij,R.P. (2017) Histone-derived piRNA biogenesis depends on the ping-pong partners Piwi5 and Ago3 in Aedes aegypti. *Nucleic Acids Res.*, **45**, 4881–4892.
44. Maringer,K., Yousuf,A., Heesom,K.J., Fan,J., Lee,D., Fernandez-Sesma,A., Bessant,C., Matthews,D.A. and Davidson,A.D. (2017) Proteomics informed by transcriptomics for characterising active transposable elements and genome annotation in Aedes aegypti. *BMC Genomics*, **18**, 101.
45. Matthews,B.J., Dudchenko,O., Kingan,S.B., Koren,S., Antoshechkin,I., Crawford,J.E., Glassford,W.J., Herre,M., Redmond,S.N., Rose,N.H. *et al.* (2018) Improved reference genome of Aedes aegypti informs arbovirus vector control. *Nature*, **563**, 501–507.
46. Gamsjaeger,R., Liew,C.K., Loughlin,F.E., Crossley,M. and Mackay,J.P. (2007) Sticky fingers: zinc-fingers as protein-recognition motifs. *Trends Biochem. Sci.*, **32**, 63–70.
47. Calabretta,S. and Richard,S. (2015) Emerging roles of disordered sequences in RNA-Binding proteins. *Trends Biochem. Sci.*, **40**, 662–672.
48. Schnettler,E., Sreenu,V.B., Mottram,T. and McFarlane,M. (2016) Wolbachia restricts insect-specific flavivirus infection in Aedes aegypti cells. *J. Gen. Virol.*, **97**, 3024–3029.
49. Aguiar,E.R.G.R., Olmo,R.P., Paro,S., Ferreira,F.V., de Faria,I.J.D., Todjro,Y.M.H., Lobo,F.P., Kroon,E.G., Meignin,C., Gatherer,D. *et al.* (2015) Sequence-independent characterization of viruses based on the pattern of viral small RNAs produced by the host. *Nucleic Acids Res.*, **43**, 6191–6206.
50. Blair,C.D. and Olson,K.E. (2015) The role of RNA interference (RNAi) in arbovirus-vector interactions. *Viruses*, **7**, 820–843.
51. Bronkhorst,A.W. and van Rij,R.P. (2014) The long and short of antiviral defense: small RNA-based immunity in insects. *Curr. Opin. Virol.*, **7**, 19–28.
52. Malone,C.D., Brennecke,J., Dus,M., Stark,A., McCombie,W.R., Sachidanandam,R. and Hannon,G.J. (2009) Specialized piRNA pathways act in germline and somatic tissues of the Drosophila ovary. *Cell*, **137**, 522–535.
53. Li,C., Vagin,V.V., Lee,S., Xu,J., Ma,S., Xi,H., Seitz,H., Horwich,M.D., Syrzycka,M., Honda,B.M. *et al.* (2009) Collapse of germline piRNAs in the absence of Argonaute3 reveals somatic piRNAs in flies. *Cell*, **137**, 509–521.
54. Sato,K., Iwasaki,Y.W., Shibuya,A., Carninci,P., Tsuchizawa,Y., Ishizu,H., Siomi,M.C. and Siomi,H. (2015) Krimper enforces an antisense bias on piRNA pools by Binding AGO3 in the Drosophila germline. *Mol. Cell*, **59**, 553–563.
55. Webster,A., Li,S., Hur,J.K., Wachsmuth,M., Bois,J.S., Perkins,E.M., Patel,D.J. and Aravin,A.A. (2015) Aub and Ago3 are recruited to nuage through two mechanisms to form a Ping-Pong complex assembled by Krimper. *Mol. Cell*, **59**, 564–575.
56. Gainetdinov,I., Colpan,C., Arif,A., Cecchini,K. and Zamore,P.D. (2018) A single mechanism of biogenesis, initiated and directed by PIWI Proteins, explains piRNA production in most animals. *Mol. Cell*, **71**, 775–790.
57. Marques,J.T., Wang,J.P., Wang,X., de Oliveira,K.P., Gao,C., Aguiar,E.R., Jafari,N. and Carthew,R.W. (2013) Functional specialization of the small interfering RNA pathway in response to virus infection. *PLoS Pathog.*, **9**, e1003579.
58. Hartig,J.V. and Forstemann,K. (2011) Loqs-PD and R2D2 define independent pathways for RISC generation in Drosophila. *Nucleic Acids Res.*, **39**, 3836–3851.
59. Wang,W., Han,B.W., Tipping,C., Ge,D.T., Zhang,Z., Weng,Z. and Zamore,P.D. (2015) Slicing and binding by Ago3 or aub trigger Piwi-Bound piRNA production by distinct mechanisms. *Mol. Cell*, **59**, 819–830.
60. Reuter,M., Chuma,S., Tanaka,T., Franz,T., Stark,A. and Pillai,R.S. (2009) Loss of the Mili-interacting Tudor domain-containing protein-1 activates transposons and alters the Mili-associated small RNA profile. *Nat. Struct. Mol. Biol.*, **16**, 639–646.
61. Campbell,C.L., Black,W.Ct., Hess,A.M. and Foy,B.D. (2008) Comparative genomics of small RNA regulatory pathway components in vector mosquitoes. *BMC Genomics*, **9**, 425.
62. Lewis,S.H., Salmela,H. and Obbard,D.J. (2016) Duplication and diversification of dipteran argonaute genes, and the evolutionary divergence of Piwi and Aubergine. *Genome Biol. Evol.*, **8**, 507–518.
63. Akbari,O.S., Antoshechkin,I., Amrhein,H., Williams,B., Diloreto,R., Sandler,J. and Hay,B.A. (2013) The developmental transcriptome of the mosquito Aedes aegypti, an invasive species and major arbovirus vector. *G3 (Bethesda)*, **3**, 1493–1509.